Available online at www.sciencedirect.com
SCIENCE DIRECT®
International Journal of Solids and Structures 42 (2005) 6261–6276
INTERNATIONAL JOURNAL OF SOLIDS and STRUCTURES
www.elsevier.com/locate/ijsolstr

Linear constitutive model for mechano-sorptive creep in paper

Johan Alfthan, Peter Gudmundson *

KTH Solid Mechanics, Royal Institute of Technology, SE-100 44 Stockholm, Sweden

Received 22 June 2004; received in revised form 31 May 2005; accepted 3 June 2005
Available online 2 August 2005

Abstract

The creep of paper is accelerated by moisture cycling. This effect is known as mechano-sorptive creep. It is assumed that this is an effect of transient stresses produced during moisture content changes in combination with non-linear creep behaviour of the fibres. The stresses produced by the moisture content changes are often much larger than the applied mechanical loads. If this is the case, the mechanical loads are only a perturbation to the internal stress state, and it will appear as if the mechano-sorptive creep is linear in stress. It is possible to take advantage of this feature. In the present report the pure moisture problem is first solved. The mechanical load is then treated as a perturbation of the solution to the moisture problem. Using this strategy, it is possible to linearize a non-linear network model for mechano-sorptive creep and to formulate a continuum model. As a result, the number of variables in the model is reduced. This is a significant improvement as it will be possible to use the linearized model to describe the material in a finite element program and solve problems with complicated geometries.

Keywords: Modeling; Mechano-sorptive creep; Moisture accelerated creep; Paper; Perturbation method

1. Introduction

Paper and board packages are often loaded for times long enough for creep to be important, and this must be considered in design. Paper is sensitive to moisture and the creep compliance increases with moisture content. High humidity climate is however not the worst possible environment as creep is also accelerated by varying humidity (Byrd, 1972a,b). The accelerated creep is known as mechano-sorptive creep, and is also found in wood (Armstrong and Kingston, 1960; Armstrong and Christensen, 1961), concrete

* Corresponding author. Fax: +46 8 411 24 18.
E-mail address: peter@hallf.kth.se (P. Gudmundson).

0020-7683/$ - see front matter © 2005 Elsevier Ltd. All rights reserved.
doi:10.1016/j.ijsolstr.2005.06.029

(Pickett, 1942) and some synthetic fibres (Wang et al., 1990, 1991, 1992, 1993; Habeger and Coffin, 2000; Habeger et al., 2001).

There is still no generally accepted explanation for mechano-sorptive creep, but there are several hypotheses and models. One possible explanation is that large local stresses are produced when the moisture content changes due to inhomogeneous hygroexpansion, which in turn will accelerate the creep if the creep rate depends non-linearly on stresses. Models have demonstrated that this mechanism will produce accelerated creep resembling the creep behaviour found in experiments (Pickett, 1942; Habeger and Coffin, 2000; Alfthan et al., 2002; Alfthan, 2003). The advantage over several other models is that no special mechanism is introduced to explain mechano-sorptive creep—it is known that the creep of fibres and paper is non-linear and inhomogeneous hygroexpansion can be the result of material inhomogeneities, moisture gradients or both. However, the non-linearity necessary for the mechanism makes the models complicated, and numerical methods are necessary even for simple problems. The network models (Alfthan et al., 2002; Alfthan, 2003) include many variables and equations to solve, and numerical simulations are therefore very slow.

In Alfthan (2003) it was found that the network model, albeit based on a non-linear mechanism, exhibited an almost linear behaviour between stresses and strains for mechanical loads that are encountered in applications. In the present paper, this feature is exploited to linearize the model, and a continuum model for mechano-sorptive creep of paper with a reduced number of variables is obtained. This linearized model can for example be implemented as a material model in a finite element program and it can be used to solve problems with more complicated geometries, for example a corrugated board container.

2. Linearization of the network model

It is assumed that the internal stresses produced by inhomogeneous hygroexpansion are much larger than the stresses produced by externally applied mechanical loads, and that the latter can be treated as a small perturbation of the former stress state. An approximate solution to a problem with moisture variations and external loads is then obtained by first solving a non-linear problem with moisture variations but no external loads, and then solve a linearized problem to get the perturbation caused by the external loads. A related analysis of moisture induced transients in DMA response of a simple one dimensional model is found in Coffin and Habeger (2001).

Fig. 1 shows the geometry of a fibre. In the following, index A is used for variables and constants for the free segments, index B is used for the bonded segments and index C is used for the bonded crossing fibres. Properties with index A or B reflect the longitudinal behaviour of fibres, while properties with index C reflect the transverse behaviour.

2.1. Analysis of the pure moisture problem

First the pure moisture problem is considered. It is assumed that the moisture content m is known as a function of time t, $m = m(t)$. It is also assumed that the free segments of the fibres can expand freely so that no stresses are created, i.e.,

$$\varepsilon_A = \beta_A m, \tag{1}$$

$$\sigma_A = 0. \tag{2}$$

For the bonded segments, see Fig. 1, strains and stresses are related by

$$\varepsilon_B = \varepsilon_C, \tag{3}$$

$$\sigma_B + \sigma_C = 0. \tag{4}$$

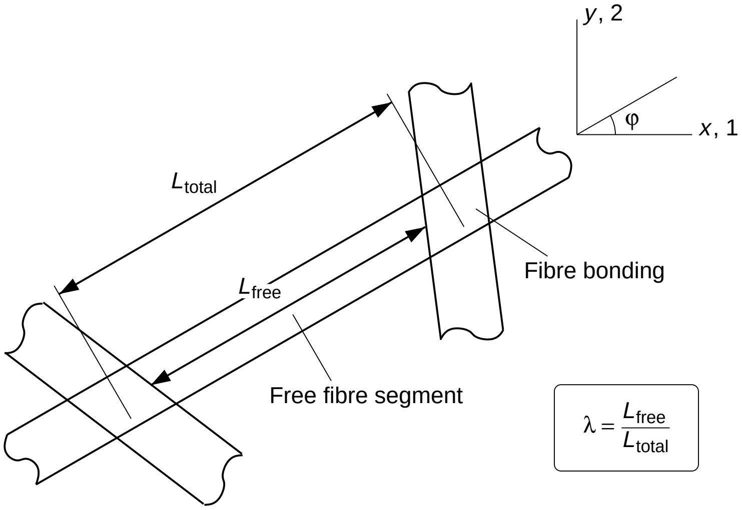

Fig. 1. Geometry of the fibre segments. The ratio λ is defined as the length of the free segments, L_{free}, divided by the total length, L_{total}, and the direction of the fibre is defined by the angle φ measured from the x-axis of the coordinate system.

where it has been assumed that fibres cross at right angles. The stresses σ_B and σ_C relax as the material creeps and will eventually vanish. The constitutive laws for the bonded fibre segments read

$$\varepsilon_B = \frac{\sigma_B}{E_B} + \varepsilon_B^c + \beta_B m, \tag{5}$$

$$\varepsilon_C = \frac{\sigma_C}{E_C} + \varepsilon_C^c + \beta_C m, \tag{6}$$

where the creep strains ε_B^c and ε_C^c are given by the creep laws

$$\dot{\varepsilon}_B^c = f_B(\sigma_B, \varepsilon_B^c), \tag{7}$$

$$\dot{\varepsilon}_C^c = f_C(\sigma_C, \varepsilon_C^c). \tag{8}$$

For a given moisture content history, Eqs. (1)–(8) constitute a non-linear system of equations for the stresses and strains of the pure moisture problem.

The average strain of a fibre will be

$$\varepsilon = \lambda \varepsilon_A + (1 - \lambda)\varepsilon_B, \tag{9}$$

where λ is the ratio between free fibre length and total fibre length, see Fig. 1. For an anisotropic fibre orientation, the ratio λ generally vary with orientation.

The average strain is also related to the macroscopic strains of the sheet. In accordance with Alfthan (2003), it is assumed that the strain of a fibre is equal to the macroscopic strain in the fibre direction, i.e.,

$$\varepsilon = \varepsilon_x \cos^2\varphi + \varepsilon_y \sin^2\varphi + \gamma_{xy} \sin\varphi \cos\varphi, \tag{10}$$

where φ is the angle of the fibre measured from the x-axis.

If the fibre distribution is given, it is possible to calculate the number of fibre crossings (Komori and Makishima, 1977), and from that the ratio λ can be calculated. For a plane fibre network, with rectangular cross sections of the fibres, the ratio λ is given by

$$\lambda = 1 - 2\rho \int_{-\pi/2}^{\pi/2} f(\psi) |\sin(\varphi - \psi)| \, d\psi, \tag{11}$$

where f is the frequency function of the fibre distribution. If the frequency function is

$$f = \frac{1}{\pi}(1 + \alpha \cos 2\varphi), \tag{12}$$

then λ will be given by

$$\lambda = \lambda_x \cos^2\varphi + \lambda_y \sin^2\varphi, \tag{13}$$

with

$$\lambda_x = 1 - \frac{4\rho}{\pi} + \frac{4\rho\alpha}{3\pi}, \tag{14}$$

$$\lambda_y = 1 - \frac{4\rho}{\pi} - \frac{4\rho\alpha}{3\pi}, \tag{15}$$

where ρ is the volume fraction of fibres in the network.

In this case the initial assumptions Eqs. (1) and (2) will be fulfilled, and Eqs. (9) and (10) will be reduced to

$$\varepsilon_x = \lambda_x \varepsilon_A + (1 - \lambda_x)\varepsilon_B, \tag{16}$$

$$\varepsilon_y = \lambda_y \varepsilon_A + (1 - \lambda_y)\varepsilon_B, \tag{17}$$

$$\gamma_{xy} = 0. \tag{18}$$

For general fibre distributions, Eqs. (1) and (2) will not be exactly satisfied, but the error is quite small.

2.2. Linearized analysis of the mechanical problem

In the following analysis, it is assumed that the mechanical load can be treated as a small perturbation to the moisture problem. The perturbation strains $\delta\varepsilon_A$, $\delta\varepsilon_B$ and $\delta\varepsilon_C$ in a fibre are then given by

$$\delta\varepsilon_A = \frac{\delta\sigma_A}{E_A} + \delta\varepsilon_A^c, \tag{19}$$

$$\delta\varepsilon_B = \frac{\delta\sigma_B}{E_B} + \delta\varepsilon_B^c, \tag{20}$$

$$\delta\varepsilon_C = \frac{\delta\sigma_C}{E_C} + \delta\varepsilon_C^c, \tag{21}$$

where $\delta\sigma_A$, $\delta\sigma_B$ and $\delta\sigma_C$ are the perturbations in stress and $\delta\varepsilon_A^c$, $\delta\varepsilon_B^c$ and $\delta\varepsilon_C^c$ are the creep strains caused by the perturbation.

The creep strains will be given by Eqs. (7) and (8) and the corresponding creep law for the free segments

$$\dot{\varepsilon}_A^c = f_A(\sigma_A, \varepsilon_A^c). \tag{22}$$

The functions f_A and f_B are equal as both are used to describe the longitudinal behaviour of the fibres.

The mechanical stresses are only a perturbation to the stress state of the pure moisture problem, so it is viable to approximate the creep laws by Taylor expansions

$$\dot{\varepsilon}_A^c \approx f_A(0,0) + \frac{\partial f_A}{\partial \sigma_A}(0,0)\delta\sigma_A + \frac{\partial f_A}{\partial \varepsilon_A^c}(0,0)\delta\varepsilon_A^c, \tag{23}$$

$$\dot{\varepsilon}_B^c \approx f_B(\sigma_B^0, \varepsilon_B^{c0}) + \frac{\partial f_B}{\partial \sigma_B}(\sigma_B^0, \varepsilon_B^{c0})\delta\sigma_B + \frac{\partial f_B}{\partial \varepsilon_B^c}(\sigma_B^0, \varepsilon_B^{c0})\delta\varepsilon_B^c, \tag{24}$$

$$\dot{\varepsilon}_C^c \approx f_C(\sigma_C^0, \varepsilon_C^{c0}) + \frac{\partial f_C}{\partial \sigma_C}(\sigma_C^0, \varepsilon_C^{c0})\delta\sigma_C + \frac{\partial f_C}{\partial \varepsilon_C^c}(\sigma_C^0, \varepsilon_C^{c0})\delta\varepsilon_C^c, \tag{25}$$

where σ_B^0, ε_B^{c0}, σ_C^0 and ε_C^{c0} are the time dependent stresses and strains that result from the pure moisture problem. Identification of the perturbations to the creep strain rates, $\delta\dot{\varepsilon}_A^c$, $\delta\dot{\varepsilon}_B^c$ and $\delta\dot{\varepsilon}_C^c$, leads to the linearized creep laws

$$\delta\dot{\varepsilon}_A^c = \frac{\partial f_A}{\partial \sigma_A}(0,0)\delta\sigma_A + \frac{\partial f_A}{\partial \varepsilon_A^c}(0,0)\delta\varepsilon_A^c, \tag{26}$$

$$\delta\dot{\varepsilon}_B^c = \frac{\partial f_B}{\partial \sigma_B}(\sigma_B^0, \varepsilon_B^{c0})\delta\sigma_B + \frac{\partial f_B}{\partial \varepsilon_B^c}(\sigma_B^0, \varepsilon_B^{c0})\delta\varepsilon_B^c, \tag{27}$$

$$\delta\dot{\varepsilon}_C^c = \frac{\partial f_C}{\partial \sigma_C}(\sigma_C^0, \varepsilon_C^{c0})\delta\sigma_C + \frac{\partial f_C}{\partial \varepsilon_C^c}(\sigma_C^0, \varepsilon_C^{c0})\delta\varepsilon_C^c. \tag{28}$$

The perturbation strains and stresses in the fibre are related by

$$\delta\varepsilon_B = \delta\varepsilon_C, \tag{29}$$

$$\delta\sigma_B + \delta\sigma_C = \delta\sigma_A = \delta\sigma, \tag{30}$$

$$\delta\varepsilon = \lambda\delta\varepsilon_A + (1-\lambda)\delta\varepsilon_B, \tag{31}$$

where $\delta\sigma$ has been introduced as a shorthand for the stress in the free segments.

Eqs. (19)–(31) can be interpreted as a linear rheological model, see Fig. 2. The parameters of the rheological model are identified from Eqs. (26)–(28)

$$\frac{1}{\eta_A} = \frac{\partial f_A}{\partial \sigma_A}(0,0), \tag{32}$$

$$\frac{1}{E_A^2} = -\frac{\partial f_A}{\partial \sigma_A}(0,0) \bigg/ \frac{\partial f_A}{\partial \varepsilon_A^c}(0,0), \tag{33}$$

$$\frac{1}{\eta_B} = \frac{\partial f_B}{\partial \sigma_B}(\sigma_B^0, \varepsilon_B^{c0}), \tag{34}$$

$$\frac{1}{E_B^2} = -\frac{\partial f_B}{\partial \sigma_B}(\sigma_B^0, \varepsilon_B^{c0}) \bigg/ \frac{\partial f_B}{\partial \varepsilon_B^c}(\sigma_B^0, \varepsilon_B^{c0}), \tag{35}$$

$$\frac{1}{\eta_C} = \frac{\partial f_C}{\partial \sigma_C}(\sigma_C^0, \varepsilon_C^{c0}), \tag{36}$$

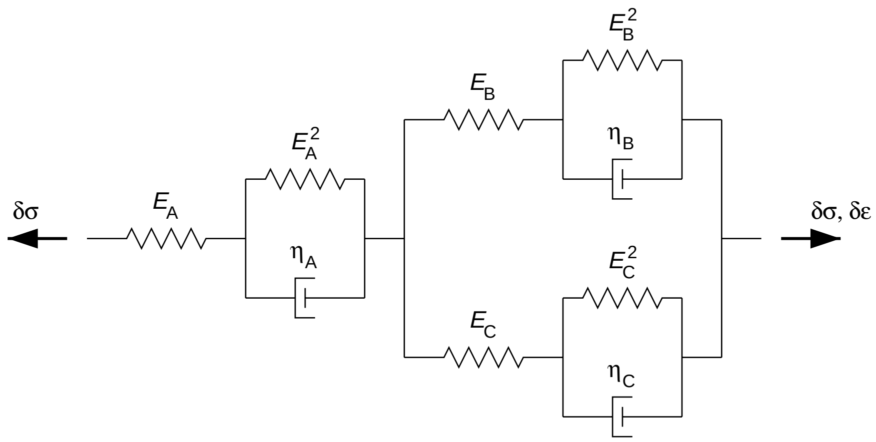

Fig. 2. A rheological model representing Eqs. (19)–(28). The parameters of the rheological model are given by Eqs. (32)–(37).

$$\frac{1}{E_{\mathrm{C}}^{2}} = -\frac{\partial f_{\mathrm{C}}}{\partial \sigma_{\mathrm{C}}}(\sigma_{\mathrm{C}}^{0}, \varepsilon_{\mathrm{C}}^{\mathrm{c0}}) \Big/ \frac{\partial f_{\mathrm{C}}}{\partial \varepsilon_{\mathrm{C}}^{\mathrm{c}}}(\sigma_{\mathrm{C}}^{0}, \varepsilon_{\mathrm{C}}^{\mathrm{c0}}). \tag{37}$$

The parameters depend on the solution from the pure moisture problem, hence they will be time dependent. Using the parameters of the rheological model, Eqs. (26)–(28) can be rewritten as

$$\delta\dot{\varepsilon}_{\mathrm{A}}^{\mathrm{c}} = \frac{\delta\sigma_{\mathrm{A}} - E_{\mathrm{A}}^{2}\delta\varepsilon_{\mathrm{A}}^{\mathrm{c}}}{\eta_{\mathrm{A}}}, \tag{38}$$

$$\delta\dot{\varepsilon}_{\mathrm{B}}^{\mathrm{c}} = \frac{\delta\sigma_{\mathrm{B}} - E_{\mathrm{B}}^{2}\delta\varepsilon_{\mathrm{B}}^{\mathrm{c}}}{\eta_{\mathrm{B}}}, \tag{39}$$

$$\delta\dot{\varepsilon}_{\mathrm{C}}^{\mathrm{c}} = \frac{\delta\sigma_{\mathrm{C}} - E_{\mathrm{C}}^{2}\delta\varepsilon_{\mathrm{C}}^{\mathrm{c}}}{\eta_{\mathrm{C}}}. \tag{40}$$

If it is assumed that the creep can be described by the non-linear creep laws

$$f_{\mathrm{A}} = a_{\mathrm{A}} \sinh(b_{\mathrm{A}}(\sigma_{\mathrm{A}} - E_{\mathrm{A}}^{\mathrm{c}}\varepsilon_{\mathrm{A}}^{\mathrm{c}})), \tag{41}$$

$$f_{\mathrm{B}} = a_{\mathrm{B}} \sinh(b_{\mathrm{B}}(\sigma_{\mathrm{B}} - E_{\mathrm{B}}^{\mathrm{c}}\varepsilon_{\mathrm{B}}^{\mathrm{c}})), \tag{42}$$

$$f_{\mathrm{C}} = a_{\mathrm{C}} \sinh(b_{\mathrm{C}}(\sigma_{\mathrm{C}} - E_{\mathrm{C}}^{\mathrm{c}}\varepsilon_{\mathrm{C}}^{\mathrm{c}})), \tag{43}$$

then

$$\frac{1}{\eta_{\mathrm{A}}} = a_{\mathrm{A}} b_{\mathrm{A}}, \tag{44}$$

$$E_{\mathrm{A}}^{2} = E_{\mathrm{A}}^{\mathrm{c}}, \tag{45}$$

$$\frac{1}{\eta_{\mathrm{B}}} = a_{\mathrm{B}} b_{\mathrm{B}} \cosh(b_{\mathrm{B}}(\sigma_{\mathrm{B}}^{0} - E_{\mathrm{B}}^{\mathrm{c}}\varepsilon_{\mathrm{B}}^{\mathrm{c0}})), \tag{46}$$

$$E_{\mathrm{B}}^{2} = E_{\mathrm{B}}^{\mathrm{c}}, \tag{47}$$

$$\frac{1}{\eta_{\mathrm{C}}} = a_{\mathrm{C}} b_{\mathrm{C}} \cosh(b_{\mathrm{C}}(\sigma_{\mathrm{C}}^{0} - E_{\mathrm{C}}^{\mathrm{c}}\varepsilon_{\mathrm{C}}^{\mathrm{c0}})), \tag{48}$$

$$E_{\mathrm{C}}^{2} = E_{\mathrm{C}}^{\mathrm{c}}, \tag{49}$$

where it has been utilized that stresses in the free segments vanish for the moisture problem.

2.3. Continuum model

In this subsection indices i, j, k and l denoted coordinate directions, and they take values 1 and 2 corresponding to x and y respectively, see Fig. 1. A repeated index letter in an expression indicates a sum over that index from 1 to 2. Using this notation, the strain of any fibre is assumed to be given by the macroscopic strains of the sheet according to

$$\delta\varepsilon = \delta\varepsilon_{kl} n_k n_l, \tag{50}$$

where $n_1 = \cos\varphi$ and $n_2 = \sin\varphi$, and the macroscopic specific stresses are given by

$$\delta\sigma_{ij}^{w} = \frac{1}{\rho_{\mathrm{f}}} \int_{-\pi/2}^{\pi/2} \delta\sigma f(\varphi) n_i n_j \,\mathrm{d}\varphi, \tag{51}$$

where ρ_{f} is the fibre density and $f(\varphi)$ is the frequency function of the fibre distribution, which must fulfill the condition

$$\int_{-\pi/2}^{\pi/2} f(\varphi)\,\mathrm{d}\varphi = 1. \tag{52}$$

Eq. (51) can alternatively be expressed in terms of the operator I_{ij} according to

$$I_{ij}(\chi) = \frac{1}{\rho_{\mathrm{f}}} \int_{-\pi/2}^{\pi/2} \chi f(\varphi) n_i n_j \,\mathrm{d}\varphi, \tag{53}$$

where χ is any function of φ, so that Eq. (51) can be written

$$\delta\sigma_{ij}^{w} = I_{ij}(\delta\sigma). \tag{54}$$

Applying the operator I_{ij} on $\delta\varepsilon$ according to Eq. (50) results in

$$I_{ij}(\delta\epsilon) = \frac{1}{\rho_{\mathrm{f}}} \int_{-\pi/2}^{\pi/2} \delta\varepsilon_{kl} f(\varphi) n_i n_j n_k n_l \,\mathrm{d}\varphi = \frac{1}{\rho_{\mathrm{f}}} C_{ijkl} \delta\varepsilon_{kl}, \tag{55}$$

where

$$C_{ijkl} = \int_{-\pi/2}^{\pi/2} f(\varphi) n_i n_j n_k n_l \,\mathrm{d}\varphi. \tag{56}$$

Eqs. (54) and (55) can be written in vector form

$$\delta\boldsymbol{\sigma}^{w} = \mathbf{I}(\delta\sigma), \tag{57}$$

$$\mathbf{I}(\delta\varepsilon) = \frac{1}{\rho_{\mathrm{f}}} \mathbf{C} \delta\boldsymbol{\varepsilon}, \tag{58}$$

where

$$\delta\boldsymbol{\sigma}^{w} = \begin{bmatrix} \delta\sigma_{11}^{w} \\ \delta\sigma_{22}^{w} \\ \delta\sigma_{12}^{w} \end{bmatrix} = \begin{bmatrix} \delta\sigma_{x}^{w} \\ \delta\sigma_{y}^{w} \\ \delta\tau_{xy}^{w} \end{bmatrix}, \tag{59}$$

$$\delta\boldsymbol{\varepsilon} = \begin{bmatrix} \delta\varepsilon_{11} \\ \delta\varepsilon_{22} \\ 2\delta\varepsilon_{12} \end{bmatrix} = \begin{bmatrix} \delta\varepsilon_{x} \\ \delta\varepsilon_{y} \\ \delta\gamma_{xy} \end{bmatrix}, \tag{60}$$

$$\mathbf{C} = \begin{bmatrix} C_{1111} & C_{1122} & C_{1112} \\ C_{2211} & C_{2222} & C_{2212} \\ C_{1211} & C_{1222} & C_{1212} \end{bmatrix}. \tag{61}$$

The operator I_{ij} can as well be applied to Eqs. (19)–(21), (38)–(40) and (29)–(31), resulting in the corresponding equations

$$\delta\boldsymbol{\varepsilon}_{\mathrm{A}} = \frac{\delta\boldsymbol{\sigma}_{\mathrm{A}}}{E_{\mathrm{A}}} + \delta\boldsymbol{\varepsilon}_{\mathrm{A}}^{\mathrm{c}}, \tag{62}$$

$$\delta\boldsymbol{\varepsilon}_{\mathrm{B}} = \frac{\delta\boldsymbol{\sigma}_{\mathrm{B}}}{E_{\mathrm{B}}} + \delta\boldsymbol{\varepsilon}_{\mathrm{B}}^{\mathrm{c}}, \tag{63}$$

$$\delta\boldsymbol{\varepsilon}_{\mathrm{C}} = \frac{\delta\boldsymbol{\sigma}_{\mathrm{C}}}{E_{\mathrm{C}}} + \delta\boldsymbol{\varepsilon}_{\mathrm{C}}^{\mathrm{c}}, \tag{64}$$

$$\delta\dot{\boldsymbol{\varepsilon}}_{\mathrm{A}}^{\mathrm{c}} = \frac{\delta\boldsymbol{\sigma}_{\mathrm{A}} - E_{\mathrm{A}}^{2}\delta\boldsymbol{\varepsilon}_{\mathrm{A}}^{\mathrm{c}}}{\eta_{\mathrm{A}}}, \tag{65}$$

$$\delta\dot{\boldsymbol{\varepsilon}}_{\mathrm{B}}^{\mathrm{c}} = \frac{\delta\boldsymbol{\sigma}_{\mathrm{B}} - E_{\mathrm{B}}^{2}\delta\boldsymbol{\varepsilon}_{\mathrm{B}}^{\mathrm{c}}}{\eta_{\mathrm{B}}}, \tag{66}$$

$$\delta\dot{\boldsymbol{\varepsilon}}_{\mathrm{C}}^{\mathrm{c}} = \frac{\delta\boldsymbol{\sigma}_{\mathrm{C}} - E_{\mathrm{C}}^{2}\delta\boldsymbol{\varepsilon}_{\mathrm{C}}^{\mathrm{c}}}{\eta_{\mathrm{C}}}, \tag{67}$$

$$\delta\boldsymbol{\varepsilon}_{\mathrm{B}} = \delta\boldsymbol{\varepsilon}_{\mathrm{C}}, \tag{68}$$

$$\delta\boldsymbol{\sigma}_{\mathrm{B}} + \delta\boldsymbol{\sigma}_{\mathrm{C}} = \delta\boldsymbol{\sigma}_{\mathrm{A}} = \delta\boldsymbol{\sigma}^{w}, \tag{69}$$

$$\frac{1}{\rho_{\mathrm{f}}}\mathbf{C}\delta\boldsymbol{\varepsilon} = \mathbf{I}(\lambda\delta\varepsilon_{\mathrm{A}}) + \mathbf{I}((1-\lambda)\delta\varepsilon_{\mathrm{B}}). \tag{70}$$

Eq. (70) contains the unevaluated expressions $\mathbf{I}(\lambda\delta\varepsilon_{\mathrm{A}})$ and $\mathbf{I}((1-\lambda)\delta\varepsilon_{\mathrm{B}})$. If λ is a constant these will be reduced to $\lambda\delta\boldsymbol{\varepsilon}_{\mathrm{A}}$ and $(1-\lambda)\delta\boldsymbol{\varepsilon}_{\mathrm{B}}$, but λ is in general a function of φ. It is however possible to evaluate the expressions if it is assumed that $\delta\varepsilon_{\mathrm{A}}$ and $\delta\varepsilon_{\mathrm{B}}$ can be written as

$$\delta\varepsilon_{\mathrm{A}} = q_{\mathrm{A}kl}n_k n_l, \tag{71}$$

$$\delta\varepsilon_{\mathrm{B}} = q_{\mathrm{B}kl}n_k n_l, \tag{72}$$

so that

$$\delta\boldsymbol{\varepsilon}_{\mathrm{A}} = \frac{1}{\rho_{\mathrm{f}}}\mathbf{C}\mathbf{q}_{\mathrm{A}}, \tag{73}$$

$$\delta\boldsymbol{\varepsilon}_{\mathrm{B}} = \frac{1}{\rho_{\mathrm{f}}}\mathbf{C}\mathbf{q}_{\mathrm{B}}. \tag{74}$$

In this case Eq. (70) can be written as

$$\frac{1}{\rho_{\mathrm{f}}}\mathbf{C}\delta\boldsymbol{\varepsilon} = \mathbf{L}\mathbf{C}^{-1}\delta\boldsymbol{\varepsilon}_{\mathrm{A}} + (\mathbf{C}-\mathbf{L})\mathbf{C}^{-1}\delta\boldsymbol{\varepsilon}_{\mathrm{B}}, \tag{75}$$

where

$$\mathbf{L} = \begin{bmatrix} L_{1111} & L_{1122} & L_{1112} \\ L_{2211} & L_{2222} & L_{2212} \\ L_{1211} & L_{1222} & L_{1212} \end{bmatrix}, \tag{76}$$

$$L_{ijkl} = \int_{-\pi/2}^{\pi/2} f(\varphi)\lambda(\varphi)n_i n_j n_k n_l\,\mathrm{d}\varphi. \tag{77}$$

The authors were not able to prove that Eq. (75) is a valid expression in general, but numerical simulations suggest that Eqs. (71) and (72) and (75) are true.

If the frequency function f is given by Eq. (12) and the length ratio λ is given by Eq. (13), then the the matrices $\mathbf{C}$ and $\mathbf{L}$ will be

$$\mathbf{C} = \frac{1}{8}\begin{bmatrix} 3+2\alpha & 1 & 0 \\ 1 & 3-2\alpha & 0 \\ 0 & 0 & 1 \end{bmatrix} \tag{78}$$

and

$$\mathbf{L} = \frac{\lambda_x}{64}\begin{bmatrix} 20+15\alpha & 4+\alpha & 0 \\ 4+\alpha & 4-\alpha & 0 \\ 0 & 0 & 4+\alpha \end{bmatrix} + \frac{\lambda_y}{64}\begin{bmatrix} 4+\alpha & 4-\alpha & 0 \\ 4-\alpha & 20-15\alpha & 0 \\ 0 & 0 & 4-\alpha \end{bmatrix}. \tag{79}$$

Eqs. (62)–(69) and (75) constitute a linear system of differential equations. Most of the variables, $\delta\boldsymbol{\varepsilon}_{\mathrm{A}}$, $\delta\boldsymbol{\varepsilon}_{\mathrm{B}}$, $\delta\boldsymbol{\varepsilon}_{\mathrm{C}}$, $\delta\boldsymbol{\varepsilon}^{\mathrm{c}}_{\mathrm{A}}$, $\delta\boldsymbol{\varepsilon}^{\mathrm{c}}_{\mathrm{B}}$, $\delta\boldsymbol{\varepsilon}^{\mathrm{c}}_{\mathrm{C}}$, $\delta\boldsymbol{\sigma}_{\mathrm{B}}$ and $\delta\boldsymbol{\sigma}_{\mathrm{C}}$, can be regarded as internal variables that can be eliminated, leaving only the applied macroscopic stresses $\delta\boldsymbol{\sigma}^{w}$ and the resulting macroscopic strains $\delta\boldsymbol{\varepsilon}$. The total strains are obtained by adding $\delta\boldsymbol{\varepsilon}$ to the strains from the moisture problem, Eqs. (16)–(18).

3. Results

In the results presented here, Eqs. (12) and (13) with λ_x and λ_y according to Eqs. (14) and (15) have been used to describe the fibre and bond distributions. The creep of the fibres are assumed to be described by Eqs. (41)–(43). The pure moisture problem, Eqs. (1)–(8), and the mechanical problem, Eqs. (62)–(69) and (75), were solved in MATLAB (2001), using standard routines for solving the differential equations.

The fibre properties depend on the moisture content. This is reflected by letting the compliances $1/E_{\mathrm{A}}$, $1/E_{\mathrm{B}}$, $1/E_{\mathrm{C}}$, a_{A}, a_{B}, a_{C}, $1/E^{\mathrm{c}}_{\mathrm{A}}$, $1/E^{\mathrm{c}}_{\mathrm{B}}$ and $1/E^{\mathrm{c}}_{\mathrm{C}}$ increase linearly with moisture m, e.g.,

$$a_{\mathrm{A}} = a_{\mathrm{A}}(m_1) + \frac{a_{\mathrm{A}}(m_2) - a_{\mathrm{A}}(m_1)}{m_2 - m_1}(m - m_1), \tag{80}$$

where m_1 and m_2 are used as reference points. They were here chosen to be 0.075 and 0.15, respectively. In the simulations, moisture content was initially 0.10, then decreased to 0.05, increased back to 0.10 etcetera. The parameters used in the simulations are shown in Table 1. The time is normalized by the cycle period T, which should be around 5 h for the parameters to be reasonable. Unless stated otherwise the fibre distribution is uniform, i.e., $\alpha = 0$ in Eq. (12).

Fig. 3 shows the total strains for different uniaxial loads, ranging from 3.3 to 13.3 kN m/kg. The agreement between the linearized model and the non-linear network model from Alfthan (2003) is excellent for small loads. For higher loads the agreement gets worse, as the applied load is no longer small compared to the stress state resulting from the pure moisture problem, Fig. 4.

If Eqs. (19)–(31) are interpreted as the linear rheological model in Fig. 2, the accelerated creep seen in Fig. 3 can be interpreted as a result of transient decreases in effective viscosities every time the moisture content changes. Fig. 5 shows that the inverse viscosities $1/\eta_{\mathrm{B}}$ and $1/\eta_{\mathrm{C}}$ have transient peaks whenever the moisture changes.

Table 1
Parameters used in the simulations

		Moisture content		
		$m = 0.075$		$m = 0.15$
$E_{\mathrm{A}} = E_{\mathrm{B}}$	[GPa]	32.0		21.3
E_{C}	[GPa]	6.40		4.27
$Ta_{\mathrm{A}} = Ta_{\mathrm{B}}$		5.00×10^{-6}		7.50×10^{-6}
Ta_{C}		25.0×10^{-6}		37.5×10^{-6}
$b_{\mathrm{A}} = b_{\mathrm{B}}$	[Pa^{-1}]		1.00×10^{-7}	
b_{C}	[Pa^{-1}]		1.00×10^{-7}	
$E^{\mathrm{c}}_{\mathrm{A}} = E^{\mathrm{c}}_{\mathrm{B}}$	[GPa]	4.00		2.67
$E^{\mathrm{c}}_{\mathrm{C}}$	[GPa]	0.800		0.533
$\beta_{\mathrm{A}} = \beta_{\mathrm{B}}$			0.030	
β_{C}			0.60	
ρ			0.50	
ρ_{f}	[kg/m^3]		1500	

Two values are given for moisture dependent parameters. The creep compliances are normalized by the moisture cycle period T.

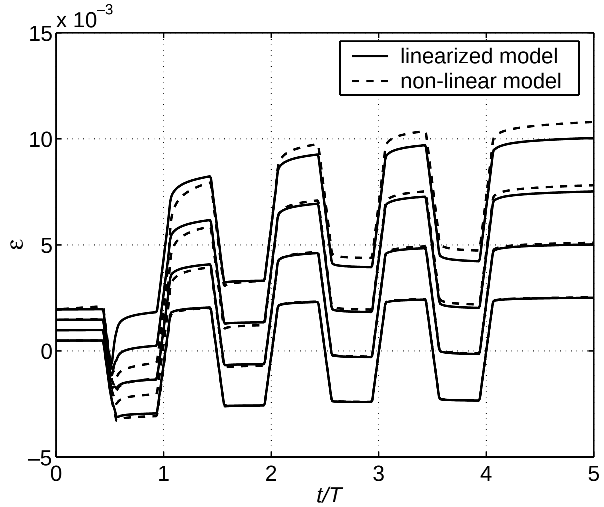

Fig. 3. Comparison between the linearized model and the full non-linear network model for different uniaxial loads. The specific stresses are 3.3 (bottom), 6.7, 10.0 and 13.3 kN m/kg (top). The agreement is excellent for small loads, but it gets worse for higher loads as the assumption behind the linearization is no longer valid.

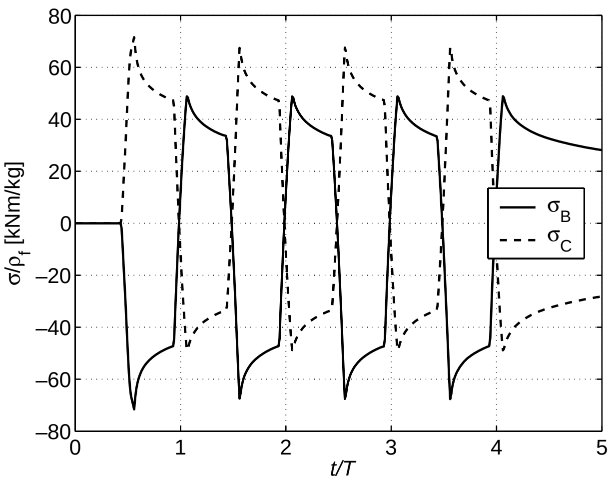

Fig. 4. The inner stresses produced by the pure moisture problem. The stresses are divided by fibre density ρ_f so it is possible to comparable them to the applied loads. The two curves show the stresses in the two different fibres at the bonds.

Figs. 6 and 7 show creep curves for different anisotropy, demonstrating the validity of Eq. (75). Fig. 6 shows uniaxial load and Fig. 7 shows a combination of uniaxial and biaxial load.

4. Conclusions and discussion

From the results it can be concluded that the agreement between the linearized model and the non-linear network model is very good for small mechanical loads, as expected from the assumptions made in the linearization. This corresponds to the linear mechano-sorptive creep behaviour often found in experiments,

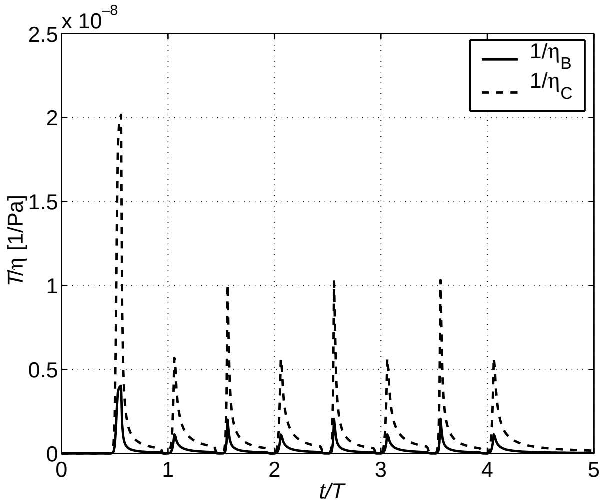

Fig. 5. The inverse viscosities $1/\eta_B$ and $1/\eta_C$ as functions of time. The effective viscosities at the bonds, η_B and η_C, are reduced every time the moisture changes resulting in the peaks shown in the plot. Due to the anisotropy of the fibres, η_C is always lower than η_B and the highest peaks corresponds to $1/\eta_C$.

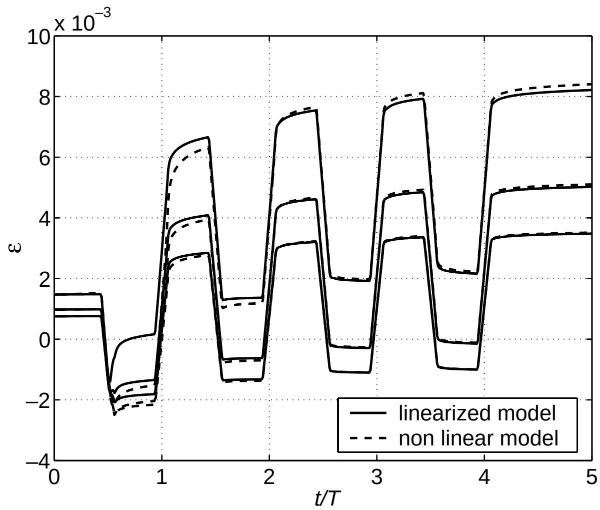

Fig. 6. Comparison between the linearized model and the full non-linear network model for different anisotropy. The load is uniaxial. The constant α in Eq. (12) is equal to −0.5 (top), 0, and +0.5 (bottom), and the specific stress is 6.7 kN m/kg.

see for example Panek et al. (2004). The linearized model is typically valid when the mechanical load is one order of magnitude smaller than the stresses produced by the moisture changes alone (Fig. 4). For higher loads the linearized model deviates more and more from the non-linear network model.

The major improvement achieved by the linearization and development of a continuum model is the speed of calculations. In the non-linear network model (Alfthan, 2003) a non-linear system of differential equations was solved for three variables in each fibre direction used in the discretization of the fibre distribution. The linearization reduces the model to a small non-linear pure moisture problem of only two

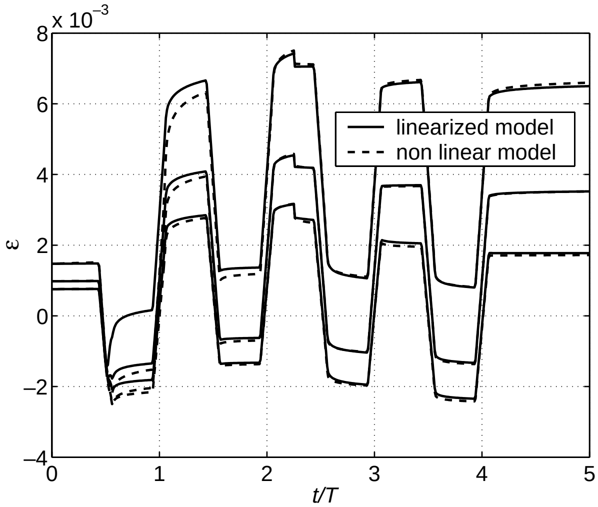

Fig. 7. Comparison between the linearized model and the full non-linear network model for different anisotropy. The load is initially uniaxial, but changes to a biaxial load at time $t/T = 2.25$. The constant α in Eq. (12) is equal to -0.5 (top), 0, and $+0.5$ (bottom), and the specific stresses are 6.7 kN m/kg.

variables and a linear mechanical problem. In the continuum formulation, the number of variables of the mechanical problem are reduced, so that only nine linear differential equations remain. In total, eleven differential equations must be solved, and of these only two are non-linear. No discretization of the fibre distribution is necessary. In comparison, 54 non-linear differential equations were solved for each result from the network model shown in Figs. 3, 6, and 7. The new model is suitable for implementation as a material model in a finite element code used for solving structural problems, like corrugated board panels or containers subjected to varying humidity and mechanical loads. In Appendix A, an implementation of the model as a user subroutine in ABAQUS (2002) is presented. The finite element formulation has been verified by comparison to MATLAB-calculations described above.

The largest problem with the model is to determine how to describe the creep, as the creep of paper and fibres is not a well-known phenomenon. Here the creep laws are assumed to have the form Eqs. (41)–(43), and parameters were chosen to get results from the simulations that resemble the creep seen in experiments. In practice it is hard to determine the parameters in these creep laws, and it is likely that other creep laws must be adopted to get an accurate description of the creep.

Acknowledgements

The financial support from Jacob Wallenbergs Forskningsstiftelse, from Lars-Erik Thunholms Stiftelse för Främjande av Vetenskaplig Forskning and from the EU project SustainPack via STFI-Packforsk is gratefully acknowledged.

The authors are also grateful to Prof. Sören Östlund for valuable comments on the manuscript.

Appendix A. Formulation for finite element analysis

In this appendix equations for finite element analysis are formulated. These equations are suitable for two dimensional solid elements or structural elements, like shells. In the following, g_t will denote a variable

g at time t, and Δg will be the change of that variable over a time increment Δt. The increment will begin at time t and end at time $t+\Delta t$. A stable time integration scheme will be obtained if central difference operators are adopted, i.e.,

$$\dot{g}_{t+\frac{1}{2}\Delta t}=\frac{\Delta g}{\Delta t}, \tag{81}$$

$$g_{t+\frac{1}{2}\Delta t}=g_t+\frac{1}{2}\Delta g. \tag{82}$$

In the commercial finite element program ABAQUS (2002) it is possible for users to define their own constitutive material models in the subroutine UMAT. In the subroutine the material Jacobian matrix, $\partial\Delta\boldsymbol{\sigma}/\partial\Delta\boldsymbol{\varepsilon}$, must be provided for the constitutive model, and stresses and inner state variables must be updated. The equations needed for the implementation of the model will be given below.

A.1. The pure moisture problem

In the pure moisture problem, there are two inner state variables that must be updated, $\varepsilon_{\mathrm{B}}^{\mathrm{c}}$ and $\varepsilon_{\mathrm{C}}^{\mathrm{c}}$. These are given by the creep laws Eqs. (7) and (8), in discrete form

$$\frac{\Delta\varepsilon_{\mathrm{B}}^{\mathrm{c}}}{\Delta t}=f_{\mathrm{B}}\left(\sigma_{\mathrm{B}t+\frac{1}{2}\Delta t},\varepsilon_{\mathrm{B}t+\frac{1}{2}\Delta t}^{\mathrm{c}}\right), \tag{83}$$

$$\frac{\Delta\varepsilon_{\mathrm{C}}^{\mathrm{c}}}{\Delta t}=f_{\mathrm{C}}\left(\sigma_{\mathrm{C}t+\frac{1}{2}\Delta t},\varepsilon_{\mathrm{C}t+\frac{1}{2}\Delta t}^{\mathrm{c}}\right), \tag{84}$$

where

$$\sigma_{\mathrm{B}t+\frac{1}{2}\Delta t}=\frac{E_{\mathrm{B}}E_{\mathrm{C}}}{E_{\mathrm{B}}+E_{\mathrm{C}}}\left(\varepsilon_{\mathrm{C}t+\frac{1}{2}\Delta t}^{\mathrm{c}}-\varepsilon_{\mathrm{B}t+\frac{1}{2}\Delta t}^{\mathrm{c}}+(\beta_{\mathrm{C}}-\beta_{\mathrm{B}})m_{t+\frac{1}{2}\Delta t}\right), \tag{85}$$

$$\sigma_{\mathrm{C}t+\frac{1}{2}\Delta t}=\frac{E_{\mathrm{B}}E_{\mathrm{C}}}{E_{\mathrm{B}}+E_{\mathrm{C}}}\left(\varepsilon_{\mathrm{B}t+\frac{1}{2}\Delta t}^{\mathrm{c}}-\varepsilon_{\mathrm{C}t+\frac{1}{2}\Delta t}^{\mathrm{c}}+(\beta_{\mathrm{B}}-\beta_{\mathrm{C}})m_{t+\frac{1}{2}\Delta t}\right), \tag{86}$$

with all material parameters evaluated for moisture content $m_{t+\frac{1}{2}\Delta t}$.

These non-linear equations for $\Delta\varepsilon_{\mathrm{B}}^{\mathrm{c}}$ and $\Delta\varepsilon_{\mathrm{C}}^{\mathrm{c}}$ can be solved using the Newton–Raphson method. The system of equations are rewritten as

$$F_{\mathrm{B}}(\Delta\varepsilon_{\mathrm{B}}^{\mathrm{c}},\Delta\varepsilon_{\mathrm{C}}^{\mathrm{c}})=\frac{\Delta\varepsilon_{\mathrm{B}}^{\mathrm{c}}}{\Delta t}-f_{\mathrm{B}}\left(\sigma_{\mathrm{B}t+\frac{1}{2}\Delta t},\varepsilon_{\mathrm{B}t+\frac{1}{2}\Delta t}^{\mathrm{c}}\right)=0, \tag{87}$$

$$F_{\mathrm{C}}(\Delta\varepsilon_{\mathrm{B}}^{\mathrm{c}},\Delta\varepsilon_{\mathrm{C}}^{\mathrm{c}})=\frac{\Delta\varepsilon_{\mathrm{C}}^{\mathrm{c}}}{\Delta t}-f_{\mathrm{C}}\left(\sigma_{\mathrm{C}t+\frac{1}{2}\Delta t},\varepsilon_{\mathrm{C}t+\frac{1}{2}\Delta t}^{\mathrm{c}}\right)=0, \tag{88}$$

and the solution is obtained by iterations using the formulas

$$\Delta\varepsilon_{\mathrm{B}n+1}^{\mathrm{c}}=\Delta\varepsilon_{\mathrm{B}n}^{\mathrm{c}}-\frac{F_{\mathrm{B}}\frac{\partial F_{\mathrm{C}}}{\partial\Delta\varepsilon_{\mathrm{C}}^{\mathrm{c}}}-\frac{\partial F_{\mathrm{B}}}{\partial\Delta\varepsilon_{\mathrm{C}}^{\mathrm{c}}}F_{\mathrm{C}}}{\frac{\partial F_{\mathrm{B}}}{\partial\Delta\varepsilon_{\mathrm{B}}^{\mathrm{c}}}\frac{\partial F_{\mathrm{C}}}{\partial\Delta\varepsilon_{\mathrm{C}}^{\mathrm{c}}}-\frac{\partial F_{\mathrm{B}}}{\partial\Delta\varepsilon_{\mathrm{C}}^{\mathrm{c}}}\frac{\partial F_{\mathrm{C}}}{\partial\Delta\varepsilon_{\mathrm{B}}^{\mathrm{c}}}}(\Delta\varepsilon_{\mathrm{B}n}^{\mathrm{c}},\Delta\varepsilon_{\mathrm{C}n}^{\mathrm{c}}), \tag{89}$$

$$\Delta\varepsilon_{\mathrm{C}n+1}^{\mathrm{c}}=\Delta\varepsilon_{\mathrm{C}n}^{\mathrm{c}}-\frac{\frac{\partial F_{\mathrm{B}}}{\partial\Delta\varepsilon_{\mathrm{B}}^{\mathrm{c}}}F_{\mathrm{C}}-F_{\mathrm{B}}\frac{\partial F_{\mathrm{C}}}{\partial\Delta\varepsilon_{\mathrm{B}}^{\mathrm{c}}}}{\frac{\partial F_{\mathrm{B}}}{\partial\Delta\varepsilon_{\mathrm{B}}^{\mathrm{c}}}\frac{\partial F_{\mathrm{C}}}{\partial\Delta\varepsilon_{\mathrm{C}}^{\mathrm{c}}}-\frac{\partial F_{\mathrm{B}}}{\partial\Delta\varepsilon_{\mathrm{C}}^{\mathrm{c}}}\frac{\partial F_{\mathrm{C}}}{\partial\Delta\varepsilon_{\mathrm{B}}^{\mathrm{c}}}}(\Delta\varepsilon_{\mathrm{B}n}^{\mathrm{c}},\Delta\varepsilon_{\mathrm{C}n}^{\mathrm{c}}), \tag{90}$$

where

$$\frac{\partial F_{\mathrm{B}}}{\partial\Delta\varepsilon_{\mathrm{B}}^{\mathrm{c}}}=\frac{1}{\Delta t}+\frac{E_{\mathrm{B}}E_{\mathrm{C}}}{2(E_{\mathrm{B}}+E_{\mathrm{C}})}\frac{\partial f_{\mathrm{B}}}{\partial\sigma_{\mathrm{B}}}-\frac{1}{2}\frac{\partial f_{\mathrm{B}}}{\partial\varepsilon_{\mathrm{B}}^{\mathrm{c}}}, \tag{91}$$

$$\frac{\partial F_{\mathrm{B}}}{\partial \Delta \varepsilon_{\mathrm{C}}^{\mathrm{c}}} = -\frac{E_{\mathrm{B}} E_{\mathrm{C}}}{2(E_{\mathrm{B}} + E_{\mathrm{C}})} \frac{\partial f_{\mathrm{B}}}{\partial \sigma_{\mathrm{B}}}, \tag{92}$$

$$\frac{\partial F_{\mathrm{C}}}{\partial \Delta \varepsilon_{\mathrm{B}}^{\mathrm{c}}} = -\frac{E_{\mathrm{B}} E_{\mathrm{C}}}{2(E_{\mathrm{B}} + E_{\mathrm{C}})} \frac{\partial f_{\mathrm{C}}}{\partial \sigma_{\mathrm{C}}}, \tag{93}$$

$$\frac{\partial F_{\mathrm{C}}}{\partial \Delta \varepsilon_{\mathrm{C}}^{\mathrm{c}}} = \frac{1}{\Delta t} + \frac{E_{\mathrm{B}} E_{\mathrm{C}}}{2(E_{\mathrm{B}} + E_{\mathrm{C}})} \frac{\partial f_{\mathrm{C}}}{\partial \sigma_{\mathrm{C}}} - \frac{1}{2} \frac{\partial f_{\mathrm{C}}}{\partial \varepsilon_{\mathrm{C}}^{\mathrm{c}}}. \tag{94}$$

A.2. The mechanical problem

From the solution to the pure moisture problem, the effective creep properties η_{A}, η_{B}, η_{C}, E_{A}^2, E_{B}^2 and E_{C}^2 can be calculated according to Eqs. (32)–(37).

The inner variables $\delta\boldsymbol{\varepsilon}_{\mathrm{A}}^{\mathrm{c}}$, $\delta\boldsymbol{\varepsilon}_{\mathrm{B}}^{\mathrm{c}}$ and $\delta\boldsymbol{\varepsilon}_{\mathrm{C}}^{\mathrm{c}}$ and the stress $\delta\boldsymbol{\sigma}^{w}$ must be updated. In finite element calculations it is preferred to use regular stresses $\delta\boldsymbol{\sigma}$ instead of specific stresses $\delta\boldsymbol{\sigma}^{w}$, so the following equations will be given for regular stresses, and the inner variables will change dimensions as appropriate. The relation between the different stresses is given by

$$\delta\boldsymbol{\sigma} = \rho\rho_{\mathrm{f}}\delta\boldsymbol{\sigma}^{w}. \tag{95}$$

The inner stresses $\delta\boldsymbol{\sigma}_{\mathrm{A}}$, $\delta\boldsymbol{\sigma}_{\mathrm{B}}$ and $\delta\boldsymbol{\sigma}_{\mathrm{C}}$ are eliminated from Eqs. (62)–(69) and (75), and the remaining equations are rewritten as

$$k_{\mathrm{A}}\Delta\delta\boldsymbol{\varepsilon}_{\mathrm{A}}^{\mathrm{c}} = \delta\boldsymbol{\sigma}_{\mathrm{A}t}^{\mathrm{eff}} + \frac{\Delta\delta\boldsymbol{\sigma}}{2}, \tag{96}$$

$$k_{\mathrm{B}}\Delta\delta\boldsymbol{\varepsilon}_{\mathrm{B}}^{\mathrm{c}} = \delta\boldsymbol{\sigma}_{\mathrm{B}t}^{\mathrm{eff}} + \frac{q_{\mathrm{B}}\Delta\delta\boldsymbol{\sigma}}{2} + \frac{k_{\mathrm{BC}}(\Delta\delta\boldsymbol{\varepsilon}_{\mathrm{C}}^{\mathrm{c}} - \Delta\delta\boldsymbol{\varepsilon}_{\mathrm{B}}^{\mathrm{c}})}{2} + \frac{\Delta k_{\mathrm{BC}}(\delta\boldsymbol{\varepsilon}_{\mathrm{C}t}^{\mathrm{c}} - \delta\boldsymbol{\varepsilon}_{\mathrm{B}t}^{\mathrm{c}})}{2}, \tag{97}$$

$$k_{\mathrm{C}}\Delta\delta\boldsymbol{\varepsilon}_{\mathrm{C}}^{\mathrm{c}} = \delta\boldsymbol{\sigma}_{\mathrm{C}t}^{\mathrm{eff}} + \frac{q_{\mathrm{C}}\Delta\delta\boldsymbol{\sigma}}{2} + \frac{k_{\mathrm{BC}}(\Delta\delta\boldsymbol{\varepsilon}_{\mathrm{B}}^{\mathrm{c}} - \Delta\delta\boldsymbol{\varepsilon}_{\mathrm{C}}^{\mathrm{c}})}{2} + \frac{\Delta k_{\mathrm{BC}}(\delta\boldsymbol{\varepsilon}_{\mathrm{B}t}^{\mathrm{c}} - \delta\boldsymbol{\varepsilon}_{\mathrm{C}t}^{\mathrm{c}})}{2}, \tag{98}$$

$$\Delta\delta\boldsymbol{\sigma} = \mathbf{J}\Delta\delta\boldsymbol{\varepsilon} - \mathbf{K}_1\Delta\delta\boldsymbol{\varepsilon}_{\mathrm{A}}^{\mathrm{c}} - q_{\mathrm{B}}\mathbf{K}_2\Delta\delta\boldsymbol{\varepsilon}_{\mathrm{B}}^{\mathrm{c}} - q_{\mathrm{C}}\mathbf{K}_2\Delta\delta\boldsymbol{\varepsilon}_{\mathrm{C}}^{\mathrm{c}} - \mathbf{K}_3\delta\boldsymbol{\sigma}_t, \tag{99}$$

where

$$k_{\mathrm{A}} = \frac{E_{\mathrm{A}}^2}{2} + \frac{\eta_{\mathrm{A}}}{\Delta t}, \tag{100}$$

$$k_{\mathrm{B}} = \frac{E_{\mathrm{B}}^2}{2} + \frac{\eta_{\mathrm{B}}}{\Delta t}, \tag{101}$$

$$k_{\mathrm{C}} = \frac{E_{\mathrm{C}}^2}{2} + \frac{\eta_{\mathrm{C}}}{\Delta t}, \tag{102}$$

$$k_{\mathrm{BC}} = \frac{E_{\mathrm{B}}E_{\mathrm{C}}}{E_{\mathrm{B}} + E_{\mathrm{C}}}, \tag{103}$$

$$q_{\mathrm{B}} = \frac{E_{\mathrm{B}}}{E_{\mathrm{B}} + E_{\mathrm{C}}}, \tag{104}$$

$$q_{\mathrm{C}} = \frac{E_{\mathrm{C}}}{E_{\mathrm{B}} + E_{\mathrm{C}}}, \tag{105}$$

$$\delta\boldsymbol{\sigma}_{\mathrm{A}t}^{\mathrm{eff}} = \delta\boldsymbol{\sigma}_{\mathrm{A}t} - E_{\mathrm{A}}^2\delta\boldsymbol{\varepsilon}_{\mathrm{A}t}^{\mathrm{c}}, \tag{106}$$

$$\delta\boldsymbol{\sigma}_{\mathrm{B}t}^{\mathrm{eff}} = \delta\boldsymbol{\sigma}_{\mathrm{B}t} - E_{\mathrm{B}}^2\delta\boldsymbol{\varepsilon}_{\mathrm{B}t}^{\mathrm{c}}, \tag{107}$$

$$\delta\boldsymbol{\sigma}_{\mathrm{C}t}^{\mathrm{eff}} = \delta\boldsymbol{\sigma}_{\mathrm{C}t} - E_{\mathrm{C}}^2\delta\boldsymbol{\varepsilon}_{\mathrm{C}t}^{\mathrm{c}}, \tag{108}$$

$$\mathbf{J} = \rho\mathbf{C}\left(\frac{\mathbf{L}}{E_{\mathrm{A}}} + \frac{\mathbf{C}-\mathbf{L}}{E_{\mathrm{B}}+E_{\mathrm{C}}}\right)^{-1}\mathbf{C}, \tag{109}$$

$$\mathbf{K}_1 = \mathbf{C}\left(\frac{\mathbf{L}}{E_{\mathrm{A}}} + \frac{\mathbf{C}-\mathbf{L}}{E_{\mathrm{B}}+E_{\mathrm{C}}}\right)^{-1}\mathbf{L}\mathbf{C}^{-1}, \tag{110}$$

$$\mathbf{K}_2 = \mathbf{C}\left(\frac{\mathbf{L}}{E_{\mathrm{A}}} + \frac{\mathbf{C}-\mathbf{L}}{E_{\mathrm{B}}+E_{\mathrm{C}}}\right)^{-1}(\mathbf{C}-\mathbf{L})\mathbf{C}^{-1}, \tag{111}$$

$$\mathbf{K}_3 = \mathbf{C}\left(\frac{\mathbf{L}}{E_{\mathrm{A}}} + \frac{\mathbf{C}-\mathbf{L}}{E_{\mathrm{B}}+E_{\mathrm{C}}}\right)^{-1}\Delta\left(\frac{\mathbf{L}}{E_{\mathrm{A}}} + \frac{\mathbf{C}-\mathbf{L}}{E_{\mathrm{B}}+E_{\mathrm{C}}}\right)\mathbf{C}^{-1}. \tag{112}$$

It is assumed that the elastic moduli E_{B} and E_{C} have similar dependencies on moisture content, so that q_{B} and q_{C} do not depend on moisture content. All other parameters must be evaluated at moisture content $m_{t+\frac{1}{2}\Delta t}$. If the moisture content changes during the increment, there will be a contribution to the equations from the changing material parameters. These contributions are found in Eqs. (97), (98) and (112), where Δ before an expression denote an incremental change of that expression.

$\mathbf{J}$ in Eq. (109) is the material Jacobian that must be provided by the material subroutine in ABAQUS (2002), i.e.,

$$\frac{\partial\Delta\delta\boldsymbol{\sigma}}{\partial\Delta\delta\boldsymbol{\varepsilon}} = \mathbf{J} = \rho\mathbf{C}\left(\frac{\mathbf{L}}{E_{\mathrm{A}}} + \frac{\mathbf{C}-\mathbf{L}}{E_{\mathrm{B}}+E_{\mathrm{C}}}\right)^{-1}\mathbf{C}. \tag{113}$$

Eqs. (96)–(99) constitute a system of linear equations, that can easily be solved. The stress increment $\Delta\delta\boldsymbol{\sigma}$ is given by

$$\begin{aligned}\Delta\delta\boldsymbol{\sigma} = {} & \left(\mathbf{I} + \frac{\mathbf{K}_1}{2k_{\mathrm{A}}} + \frac{(2q_{\mathrm{B}}^2k_{\mathrm{C}} + 2q_{\mathrm{C}}^2k_{\mathrm{B}} + k_{\mathrm{BC}})\mathbf{K}_2}{2(2k_{\mathrm{B}}k_{\mathrm{C}} + (k_{\mathrm{B}}+k_{\mathrm{C}})k_{\mathrm{BC}})}\right)^{-1}\left(\mathbf{J}\Delta\delta\boldsymbol{\varepsilon} - \frac{\mathbf{K}_1\delta\boldsymbol{\sigma}_{\mathrm{A}t}^{\mathrm{eff}}}{k_{\mathrm{A}}} - \frac{(2q_{\mathrm{B}}k_{\mathrm{C}} + k_{\mathrm{BC}})\mathbf{K}_2\delta\boldsymbol{\sigma}_{\mathrm{B}t}^{\mathrm{eff}}}{2k_{\mathrm{B}}k_{\mathrm{C}} + (k_{\mathrm{B}}+k_{\mathrm{C}})k_{\mathrm{BC}}}\right.\\ & \left. - \frac{(2q_{\mathrm{C}}k_{\mathrm{B}} + k_{\mathrm{BC}})\mathbf{K}_2\delta\boldsymbol{\sigma}_{\mathrm{C}t}^{\mathrm{eff}}}{2k_{\mathrm{B}}k_{\mathrm{C}} + (k_{\mathrm{B}}+k_{\mathrm{C}})k_{\mathrm{BC}}} - \frac{(q_{\mathrm{B}}k_{\mathrm{C}} - q_{\mathrm{C}}k_{\mathrm{B}})\Delta k_{\mathrm{BC}}\mathbf{K}_2(\delta\boldsymbol{\varepsilon}_{\mathrm{C}t}^{\mathrm{c}} - \delta\boldsymbol{\varepsilon}_{\mathrm{B}t}^{\mathrm{c}})}{2k_{\mathrm{B}}k_{\mathrm{C}} + (k_{\mathrm{B}}+k_{\mathrm{C}})k_{\mathrm{BC}}} - \mathbf{K}_3\delta\boldsymbol{\sigma}_t\right).\end{aligned} \tag{114}$$

The increments of the inner variables are

$$\Delta\delta\boldsymbol{\varepsilon}_{\mathrm{A}}^{\mathrm{c}} = \frac{\delta\boldsymbol{\sigma}_{\mathrm{A}t}^{\mathrm{eff}}}{k_{\mathrm{A}}} + \frac{\Delta\delta\boldsymbol{\sigma}}{2k_{\mathrm{A}}}, \tag{115}$$

$$\begin{aligned}\Delta\delta\boldsymbol{\varepsilon}_{\mathrm{B}}^{\mathrm{c}} = {} & \frac{(2k_{\mathrm{C}} + k_{\mathrm{BC}})\delta\boldsymbol{\sigma}_{\mathrm{B}t}^{\mathrm{eff}} + k_{\mathrm{BC}}\delta\boldsymbol{\sigma}_{\mathrm{C}t}^{\mathrm{eff}} + k_{\mathrm{C}}\Delta k_{\mathrm{BC}}(\delta\boldsymbol{\varepsilon}_{\mathrm{C}t}^{\mathrm{c}} - \delta\boldsymbol{\varepsilon}_{\mathrm{B}t}^{\mathrm{c}})}{2k_{\mathrm{B}}k_{\mathrm{C}} + (k_{\mathrm{B}}+k_{\mathrm{C}})k_{\mathrm{BC}}}\\ & + \frac{(2q_{\mathrm{B}}k_{\mathrm{C}} + k_{\mathrm{BC}})\Delta\delta\boldsymbol{\sigma}}{2(2k_{\mathrm{B}}k_{\mathrm{C}} + (k_{\mathrm{B}}+k_{\mathrm{C}})k_{\mathrm{BC}})},\end{aligned} \tag{116}$$

$$\begin{aligned}\Delta\delta\boldsymbol{\varepsilon}_{\mathrm{C}}^{\mathrm{c}} = {} & \frac{k_{\mathrm{BC}}\delta\boldsymbol{\sigma}_{\mathrm{B}t}^{\mathrm{eff}} + (2k_{\mathrm{B}} + k_{\mathrm{BC}})\delta\boldsymbol{\sigma}_{\mathrm{C}t}^{\mathrm{eff}} + k_{\mathrm{B}}\Delta k_{\mathrm{BC}}(\delta\boldsymbol{\varepsilon}_{\mathrm{B}t}^{\mathrm{c}} - \delta\boldsymbol{\varepsilon}_{\mathrm{C}t}^{\mathrm{c}})}{2k_{\mathrm{B}}k_{\mathrm{C}} + (k_{\mathrm{B}}+k_{\mathrm{C}})k_{\mathrm{BC}}}\\ & + \frac{(2q_{\mathrm{C}}k_{\mathrm{B}} + k_{\mathrm{BC}})\Delta\delta\boldsymbol{\sigma}}{2(2k_{\mathrm{B}}k_{\mathrm{C}} + (k_{\mathrm{B}}+k_{\mathrm{C}})k_{\mathrm{BC}})}\end{aligned} \tag{117}$$

with $\Delta\delta\boldsymbol{\sigma}$ according to Eq. (114).

References

ABAQUS, 2002. ABAQUS User's Manual Version 6.3. Hibbitt, Karlsson & Sorensen, Inc., Pawtucket, Rhode Island.
Alfthan, J., 2003. A simplified network model for mechano-sorptive creep in paper. J. Pulp Paper Sci. 29 (7), 228–234.

Alfthan, J., Gudmundson, P., Östlund, S., 2002. A micro-mechanical model for mechano-sorptive creep in paper. J. Pulp Paper Sci. 28 (3), 98–104.

Armstrong, L.D., Christensen, G.N., 1961. Influence of moisture changes on deformation of wood under stress. Nature 191 (4791), 869–870.

Armstrong, L.D., Kingston, R.S.T., 1960. Effect of moisture changes on creep in wood. Nature 185 (4718), 862–863.

Byrd, V.L., 1972a. Effect of relative humidity changes during creep on handsheet paper properties. Tappi 55 (2), 247–252.

Byrd, V.L., 1972b. Effect of relative humidity changes on compressive creep response of paper. Tappi 55 (11), 1612–1613.

Coffin, D.W., Habeger, C.C., 2001. The mechanics of sorption-induced transients in the loss tangent. J. Pulp Paper Sci. 27 (11), 385–390.

Habeger, C.C., Coffin, D.W., 2000. The role of stress concentrations in accelerated creep and sorption-induced physical aging. J. Pulp Paper Sci. 26 (4), 145–157.

Habeger, C.C., Coffin, D.W., Hojjatie, B., 2001. Influence of humidity cycling parameters on the moisture-accelerated creep of polymeric fibers. J. Polym. Sci. Part B Polym. Phys. 39 (17), 2048–2062.

Komori, T., Makishima, K., 1977. Numbers of fiber-to-fiber contacts in general fiber assemblies. Text. Res. J. 47 (1), 13–17.

MATLAB, 2001. MATLAB 6.1. The MathWorks, Inc., Natick, Massachusetts.

Panek, J., Fellers, C., Haraldsson, T., 2004. Principles of evaluation for the creep of paperboard in constant and cyclic humidity. Nord. Pulp Pap. Res. J. 19 (2), 155–163.

Pickett, G., 1942. The effect of change in moisture-content of the creep of concrete under a sustained load. J. Am. Concr. Inst. 13 (4), 333–355.

Wang, J.Z., Davé, V., Glasser, W., Dillard, D.A., 1993. The effects of moisture sorption on the creep behavior of fibers and composite materials. In: Harris, C., Gates, T. (Eds.), High Temperature and Environmental Effects on Polymeric Composites, vol. 1174, ASTM STP. ASTM, pp. 186–200.

Wang, J.Z., Dillard, D.A., Kamke, F.A., 1991. Transient moisture effects in materials. J. Mater. Sci. 26, 5113–5126.

Wang, J.Z., Dillard, D.A., Ward, T.C., 1992. Temperature and stress effect on the creep of aramid fibers under transient moisture conditions and discussions on the mechanism. J. Polym. Sci. Part B Polym. Phys. 30, 1391–1400.

Wang, J.Z., Dillard, D.A., Wolcott, M.P., Kamke, F.A., Wilkes, G.L., 1990. Transient moisture effect in fibers and composite materials. J. Compos. Mater. 24, 994–1009.